Atmos. Chem. Phys. Discuss., 15, 16141–16174, 2015
www.atmos-chem-phys-discuss.net/15/16141/2015/
doi:10.5194/acpd-15-16141-2015

Atmospheric Chemistry and Physics Discussions

Challenges of parameterizing CCN due to changes in particle physicochemical properties: implications from observations at a suburban site in China

F. Zhang[1,2], Z. Li[1,2,3], Y. Li[1,2], Y. Sun[4], Z. Wang[5], L. Sun[6], M. Cribb[3], C. Zhao[1,2], P. Li[1,2], and Q. Wang[4]

[1]State Key Laboratory of Earth Surface Processes and Resource Ecology, College of Global Change and Earth System Science, Beijing Normal University, Beijing 100875, China
[2]Joint Center for Global Change Studies, Beijing 100875, China
[3]Earth System Science Interdisciplinary Center and Department of Atmospheric and Oceanic Science, University of Maryland, College Park, MD, USA
[4]State Key Laboratory of Atmospheric Boundary Layer Physics and Atmospheric Chemistry, Institute of Atmospheric Physics, Chinese Academy of Sciences, Beijing 100029, China
[5]Key Laboratory of Atmospheric Composition and Optical Radiation, Anhui Institute of Optics and Fine Mechanics, Chinese Academy of Sciences, Hefei 230031, China
[6]Key Laboratory of Middle Atmosphere and Global Environment Observation (LAGEO), Institute of Atmospheric Physics, Chinese Academy of Sciences, Beijing, 100029, China

Received: 14 May 2015 – Accepted: 27 May 2015 – Published: 15 June 2015

Correspondence to: Z. Li (zli@atmos.umd.edu)

Published by Copernicus Publications on behalf of the European Geosciences Union.

Abstract

This study is concerned with the challenges of parameterizing cloud condensation nuclei (CCN) when changes in particle physicochemical properties occur, based on field measurements made at two distinct locations in China. The CCN nucleation efficiency of aerosols produced by local biomass burning was low. This is because the particles were freshly emitted with low oxidation level organics and thus are less hygroscopic. The CCN activation efficiency was enhanced significantly when the site was under the influence of air transported from far away, during which aerosol properties changed with more hygroscopic secondary organic and inorganic components. The influence of the variation in particle number size distribution (PSD) on estimating CCN number concentrations (N_{CCN}) was examined, showing poor correlation (slope = 0.8, R^2 = 0.35) of predicted and measured N_{CCN}. While the PSD is found to play a dominant role in predicting (N_{CCN}), a strong dependence of N_{CCN} on the mass fraction of organics (x_{org}) was also noted. N_{CCN} was underestimated by 52 and 13 % at supersaturation levels of 0.13 and 0.76 %, respectively, when x_{org} = 66 %. N_{CCN} was slightly overestimated, or in good agreement, with observations when x_{org} was reduced to 35 % (R^2 = 0.94). The applicability of the CCN activation spectrum obtained at Xinzhou to the Xianghe site, about 400 km to the northeast of Xinzhou, was investigated, with the goal of further examining the sensitivity of CCN to aerosol type. Overall, the mean CCN efficiency spectrum derived from Xinzhou performs well at Xianghe when the supersaturation levels are > 0.2 % (overestimation of 2–4 %). However, N_{CCN} was overestimated by ~ 20 % at supersaturation levels of < 0.1 %. This suggests that the overestimation is mainly due to the smaller proportion of aged and oxidized organic aerosols present at Xianghe compared with Xinzhou.

1 Introduction

To reduce the uncertainty of aerosol indirect effects on the radiative balance of the atmosphere, it is important to gain a good knowledge of the ability of aerosol particles to form cloud condensation nuclei (CCN) at the typical supersaturations found in the atmosphere. The CCN activity of aerosol particles is governed by the Köhler theory (Köhler, 1936). This theory determines CCN from aerosol particle size and physicochemical properties, which include the molar volume, activity coefficient, and effect on surface tension (McFiggans et al., 2006). These properties, however, are difficult to measure.

Researchers have proposed single-parameter models to parameterize the CCN activation and hygroscopicity of multi-component aerosols (Hudson and Da, 1996; Rissler et al., 2006; Petters and Kreidenweis, 2007; Wex et al., 2007). Field experiments have been conducted with the aim of better characterizing particle physicochemical parameters influencing cloud CCN activation. Due to the large spatial variability of aerosol types and compositions, the CCN activation efficiency varies greatly over different regions. CCN number concentrations (N_{CCN}) can often be better predicted in the background atmosphere (Chuang et al., 2000; Dusek et al., 2003; VanReken et al., 2003; Rissler et al., 2004; Gasparini et al., 2006; Stroud et al., 2007; Bougiatioti et al., 2009).

The largest errors are associated with urban emissions (Sotiropoulou et al., 2007). This is likely due to the organics component of aerosol particles, which have the largest uncertainty and are not fully understood. Biomass burning aerosols and secondary organics formed from the oxidation of common biogenic emissions are often more difficult to activate (Mircea et al., 2005; VanReken et al., 2005; Lee et al., 2006; Varutbangkul et al., 2006; Clarke et al., 2007; Rose et al., 2010; Engelhart et al., 2012; Paramonov et al., 2013; Lathem et al., 2013; Mei et al., 2013b; Zhang et al., 2014). Particles with aged/oxidized secondary organic components (e.g., organic acids) have been shown to be more hygroscopic (Raymond and Pandis, 2002; Hartz et al., 2006; Bougiatioti et al., 2011), but still much less hygroscopic than inorganic species. The sensitivity of

predicted N_{CCN} to organics have been examined in a number of recent studies (Wang et al., 2008; Reutter et al., 2009; Ervens et al., 2010; Kammermann et al., 2010; Ward et al., 2010; Zhang et al., 2012; Mei et al., 2013a). It is widely known that the predicted N_{CCN} is sensitive to changes in organics due to the latter's complex components. The amounts and hygroscopicity parameter of organics (κ_{org}) vary substantially and lead to significant biases in predicting CCN concentrations and aerosol indirect forcing (Sotiropoulou et al., 2007; Hings et al., 2008; Liu and Wang, 2010). Therefore, field investigations regarding CCN activity and organics impacts, especially in heavily polluted regions, are pivotal to better parameterize CCN in climate models.

Northern China is a fast developing and densely populated region of China, where aerosol loading is high (Li et al., 2007, 2011), the particle composition is complex, and severe haze pollution episodes are common (Guo et al., 2014). In recent years, CCN measurements have been collected during field campaigns carried out in the region (Wiedensohler et al., 2009; Gunthe et al., 2011; Yue et al., 2011; Deng et al., 2011, 2013; Zhang et al., 2014). These studies have presented different perspectives on the influence of particle size and composition on CCN activity. For example, Deng et al. (2013) evaluated various schemes for CCN parameterization and recommended that the particle number size distribution (PSD) together with inferred mean size-resolved activation ratios can be used to predict CCN number concentrations without considering the impact of particle composition. However, Zhang et al. (2014) demonstrated that the 30–40 % uncertainties in N_{CCN} are mainly associated with changes in particle composition. None of the above-mentioned studies have investigated the impact of organics on estimating N_{CCN} in Northern China. Zhang et al. (2012) noted a more significant influence of organics on CCN activity, but the campaign average mass fraction of organics in their study was < 20 %.

The aim of this paper is to examine the sensitivity of changes in aerosol physicochemical properties (especially aerosols containing large amounts of organics) to CCN activity, and to see how much uncertainty is incurred by applying the CCN efficiency spectra measured at one site to another site in a heavily polluted region. The

instrumentation and data used in the study are described in Sect. 2. The method for calculating the hygroscopicity parameter (κ_{chem}) is introduced in Sect. 3. The sensitivity of aerosol particle size distribution and the mass fraction of organics (x_{org}) to CCN activity, as well as the ability of the CCN efficiency spectrum observed at the Xinzhou site to represent CCN at the Xianghe site, are presented and discussed in Sect. 4. Conclusions from the study are given in Sect. 5.

2 Measurements and data

An intensive observation period field campaign similar to the Aerosol-CCN-Cloud Closure Experiment (Zhang et al., 2014), called the Atmosphere, Aerosol, Cloud, and CCN (A^2C^2) experiment, was conducted from 22 July to 26 August of 2014 at Xinzhou (38.24° N, 112.43° E; 1500 m a.s.l.), a city with a population of 0.51 million in Northern China. The site is located about 360 km southwest of the metropolitan Beijing area and about 10 km south of the local town center. The site is surrounded by agricultural land (e.g., corn) with relatively little pollution from motor vehicles and industrial activities. Sitting between two mountains (Taihang Mountain to the east and Lüliang Mountain to the west), the site experiences frequent pollution plumes from Xinzhou City to the north and from Taiyuan City to the south, the capital of Shanxi Province. Air masses from the northeast and southwest dominate over the site during summer. Depending on the wind direction, measurements at the Xinzhou site can detect pollutants of urban, rural, or mixed origins, including both fresh biomass burning emissions and aged aerosols from advection.

2.1 Instruments and measurements

During the field campaign, a Scanning Mobility Particle Sizer (SMPS), combined with a Droplet Measurement Technologies-Cloud Condensation Nuclei Counter (DMT-CCNc) (Lance et al., 2006), was used for size-resolved CCN measurements as well as

size distribution measurements. The measured aerosol PSD is within the size range of 14–600 nm. Aerosol chemical composition was measured simultaneously by an Aerodyne Aerosol Chemical Speciation Monitor (ACSM) (Sun et al., 2012).

The aerosol inlet for the size distribution measurements was equipped with a TSI Environmental Sampling System (Model 3031200), which consists of a sharp-cut PM_1 cyclone and a bundled nafion dryer. The size-resolved CCN efficiency spectra were measured by coupling the DMT-CCN_C used with the SMPS (Rose et al., 2008). In this step, the particles are rapidly dried with RH < 30 % upon entering the Differential Mobility Analyzer (DMA). Thus, size selection is effectively performed under dry conditions. Relative deviations in particle diameter should be < 1 % except for potential kinetic limitations (Mikhailov et al., 2009). The sample flow exiting the DMA was split into two parts: 0.3 L min^{-1} for the CPC and 0.5 L min^{-1} for the CCN counter (CCN_C). The DMA, controlled by TSI-AIM software, scanned one size distribution every five minutes. The CCN_C was operated at a total flow rate of 0.5 L min^{-1} with a sheath-to-aerosol flow ratio of 10. The inlet RH for CCNc was < 30 %. During the field campaign, the mean sample temperature and pressure measured by CCN_C sensors was (24.3 ± 1.4) °C and (898.4 ± 11.7) hPa. The supersaturations levels of CCN_C were calibrated with ammonium sulfate before and after the field campaign, following the procedures outlined in Rose et al. (2008). During each CCN measurement cycle, calibrated effective supersaturations were set at 0.075, 0.13, 0.17, 0.39, and 0.75 %. The overall error (1σ) for the supersaturation levels was estimated to be < 3.5 %. The completion of a full measurement cycle took 50 min (10 min for each supersaturation level).

The measurement of non-refractory submicron aerosol species including organics, sulfate, nitrate, ammonium, and chloride were made with an ACSM. During the field campaign, ambient aerosols were drawn inside through a 1/2 inch (outer diameter) stainless steel tube at a flow rate of ~ 3 L min^{-1}, of which ~ 84 cc min^{-1} was subsampled into the ACSM. An URG cyclone (Model: URG-2000-30ED) was also positioned in front of the sampling inlet to remove coarse particles with a cut-off size of 2.5 mm. Before sampling into the ACSM, aerosol particles were dried using a silica gel

desiccant. The residence time in the sampling tube was ~ 5 s. The ACSM was operated at a time resolution of ~ 15 min with a scan rate of mass spectrometer at 500 ms amu^{-1} from m/z 10 to 150. Regarding the calibration of the ACSM, mono-dispersed, size-selected 300 nm ammonium nitrate particles within a range of concentrations were sampled into both the ACSM and a condensation particle counter (CPC). The ionization efficiency (IE) was then determined by comparing the response factors of the ACSM to the mass calculated with known particle size and number concentrations from the CPC. More detailed descriptions of the operation and calibration of the ACSM are given in Sun et al. (2012) and Ng et al. (2011).

In addition to the ACSM, the black carbon (BC) in $PM_{2.5}$ was simultaneously measured at a time resolution of 5 min by a seven-wavelength aethalometer (Model AE31, Magee Scientific Corporation). The campaign averaged mass concentration of BC is ~ 2.5 μg m^{-3}. During the experiment, the campaign area was generally hot and dry, with an average temperature of 21.6 °C and an average ambient RH of 69.5 %.

2.2 Data

The raw CCN data were first filtered according to instrument recorded parameters (e.g., temperature and flow). For example, if the relative difference between the actual and preset sample flows was larger than 4 %, the data are flagged as invalid. The data is also excluded if the temperature stability was zero. These flagged data are not used for further analysis. A multiple charge correction and transfer function (Deng et al., 2011) is applied to each aerosol number (CN) size distribution spectrum as well as to the CCN efficiency spectrum. The CCN activation ratio (AR) is the ratio of N_{CCN} to CN concentration (N_{CN}).

Size-resolved CCN and PSD data, measured with a DMT-CCNc and a SMPS (with a particle size range of 10–700 nm) on 7–21 July 2013 at Xianghe (Zhang et al., 2014), are used in this study for comparisons with CCN activity at the Xinzhou site. To estimate N_{CCN} at the Xianghe site, CCN size distributions were calculated by multiplying the fitted campaign-averaged CCN efficiency spectrum obtained using the three-parameter

cumulative distribution function method (Rose et al., 2008) with the CN size distribution. The total N_{CCN} was then obtained by integrating the size-resolved N_{CCN} over the whole size range. Aerosol mass concentrations were processed using the ACSM standard data analysis software (version 1.5.3.0). Detailed procedures for the data analysis have been described by Ng et al. (2011) and Sun et al. (2012).

3 Derivation of κ_{chem}

As proposed by Petters and Kreidenweis (2007), κ can be used to describe the ability of particles to absorb water vapor and act as CCN. Based on Köhler theory (Köhler, 1936), κ relates the dry diameter of aerosol particles to the critical water vapor supersaturations. According to measurements and thermodynamic models, κ is zero for insoluble materials like soot or mineral dust. However, their hygroscopicity changes due to the aging process, so the κ value then becomes > 0. The magnitude of κ is ∼ 0.1 for secondary organic aerosols, ∼ 0.6 for ammonium sulfate and nitrate, 0.95–1 for sea salt (Niedermeier et al., 2008), and 1.28 for sodium chloride aerosols. In this study, we calculate κ_{chem} based on bulk chemical composition observations made during the field campaign. The method to derive κ_{chem} is described below.

For a given internal mixture, κ_{chem} can be predicted using a simple mixing rule based on chemical volume fractions, ε_i (Petters and Kreidenweis, 2007):

$$\kappa_{chem} = \sum_i \varepsilon_i \kappa_i \quad (1)$$

where κ_i and ε_i are the hygroscopicity parameter and volume fraction, respectively, for the individual (dry) components in the mixture and i is the number of components in the mixture. We derived ε_i from the particle chemical composition measured by the ACSM. Measurements from the ACSM show that the composition of submicron particles was dominated by organics, followed by sulfate, ammonium, and nitrate. The contribution of chloride was negligible (volume fraction of about < 2 %). The analysis of the anion

and cation balance suggests that anionic species (NO_3^-, SO_4^{2-}) were essentially neutralized by NH_4^+ over the relevant size range. For refractory species, BC represented a negligible fraction of the total submicron aerosol volume (< 3 %). Sea salt and dust are usually coarse mode particles with particle sizes > 1 µm (Whitby, 1978). The contribution of such types of aerosols is thus expected to be negligible for sizes < 1000 nm. Therefore, the submicron particles measured by the ACSM mainly consisted of organics, $(NH_4)_2SO_4$, and NH_4NO_3. The particle hygroscopicity is thus the volume average of the three participating species:

$$\kappa_{chem} = \kappa_{Org}\varepsilon_{Org} + \kappa_{(NH_4)_2SO_4}\varepsilon_{(NH_4)_2SO_4} + \kappa_{NH_4NO_3}\varepsilon_{NH_4NO_3} \quad (2)$$

The values of κ are 0.67 and 0.61 for $(NH_4)_2SO_4$ and NH_4NO_3, respectively, which have been derived from previous laboratory experiments (Petters and Kreidenweis, 2007). The following linear function derived by Mei et al. (2013) was used to estimate κ_{Org} in our study: $\kappa_{Org} = 2.10 \times f_{44} - 0.11$, where f_{44} is the fraction of m/z 44 in total organics. The mean value of κ_{Org} during the field campaign is 0.115 ± 0.019. The volume fractions of species were derived from mass concentrations and densities of participating species. The densities of $(NH_4)_2SO_4$ and NH_4NO_3 are 1770 and 1720 kg m^{-3}, respectively. The density of organics is 1200 kg m^{-3} (Turpin et al., 2001).

4 Results and discussion

4.1 CCN efficiency spectra

During the field campaign at the Xinzhou site, ∼ 790 size-resolved CCN efficiency spectra at five supersaturation levels ranging from 0.075 to 0.76 % were measured. Figure 1 shows campaign averaged spectra of the measured CCN efficiency at Xinzhou for supersaturation levels of 0.075, 0.13, 0.17, 0.39, and 0.76 %. The observed CCN efficiency at the Xianghe site is also shown. The right panels show the mass concentration fraction of particle chemical compositions at Xinzhou (top panel) and Xianghe

(bottom panel) during their respective observation periods. Significant differences in size-resolved CCN efficiency spectra at the two sites are seen. Aerosol particles at Xinzhou activate more efficiently (higher values of AR) at a given particle diameter (D_p) for the same supersaturation level. In the other words, a larger D_p was required to reach the same activation efficiency at Xianghe. This suggests that aerosol properties at each site differ.

The slope of AR with respect to diameters near D_p when AR = 50 % (defined here as the cut-off diameter, D_{cut}) provides information about the heterogeneity of the composition for size-resolved particles. For an ideal case when all CCN-active particles have the same composition and size, a steep change in AR from 0 to 1 would be observed as D_p reached D_{cut}. A gradual increase in size-resolved AR with D_p suggests that aerosol particles have different hygroscopicities. The steeper slopes of AR around D_{cut} observed at Xinzhou suggest that the particle composition was less heterogeneous with more hygroscopicity than particles at the Xianghe site. This can be partially explained by the magnitudes of the mean κ_{chem} at the two sites (0.42 at Xinzhou and 0.38 at Xianghe). The f_{44} is greater at Xinzhou than at Xianghe. The m/z 44 signal is mostly due to acids (Takegawa et al., 2007; Duplissy et al., 2011) or acid-derived species, such as esters. f_{44} is closely related to the organic oxidation level (Aiken et al., 2008). Oxidized/aged acids are generally more hygroscopic and easily activated. Moreover, the primary inorganic particles at the Xinzhou site are sulfates, with a mass fraction that is two times greater than that measured at Xianghe. Therefore, particles at the Xinzhou site consist of more hygroscopic sulfate-dominant inorganics and aged/oxidized secondary organics and can thus be more efficiently activated at a given D_p, as shown in Fig. 1.

4.2 Air mass influences on aerosol activity: a case study

Because air mass back trajectories combined with ambient air measurements can be used for analyzing large-scale air pollutant transport and source identification at a receptor site (Stohl, 1996; Rousseau et al., 2004), in this study, we calculated five-day

(120 h) back trajectories using the Hybrid Single-Particle Lagrangian Integrated Trajectory (HYSPLIT) model (Draxler and Hess, 1998) with National Centers for Environmental Prediction (NCEP) reanalysis data. TrajStat software (Wang et al., 2009) has been used to calculate trajectories. The arrival height of the trajectories at the Xinzhou site was at the surface.

Three cases were selected to study air mass influences on aerosol activity: (1) Case 1, 19 August 2014, 19:00–21:00 local time (LT), (2) Case 2, 9 August 2014, 03:00–10:00 LT; and (3) Case 3, 29 July 2014, 00:00–12:00 LT. Each case is associated with a different CCN efficiency spectrum, i.e., top, middle, and bottom panels of Fig. 2 are for Cases 1, 2, and 3, respectively. Their respective back trajectories are shown in Fig. 3.

In Case 1, air trajectories (red line in Fig. 3) originated from the southwest and passed through northern Shaanxi Province and northwestern Shanxi Province, then rounded back to the site from the north/northeast. So, aerosols in this case are closely associated with air parcels north/northeast of the site. The trajectories were very short, suggesting that the air flow was slow during the observational period. Under these circumstances, aerosol loading would be largely impacted by local sources around the site.

A high mass fraction of organics (> 60 %) with low f_{44} (~ 10 %) and κ_{chem} (< 0.3) values was measured during the observational period. Furthermore, the PSD showed one peak mode with D_p = 56 nm and a high N_{CN} (~ 1.7×10^4 cm^{-3}), but low mass concentration of PM_1 (28.36 µg m^{-3}). This suggests that particles were mainly composed of freshly emitted biomass burning primary organic aerosols. This type of aerosol usually originates from local emissions and is less hygroscopic with a single peak mode primarily composed of fine particles (Whitby, 1978; Hussein et al., 2005). These aerosols cannot activate efficiently. The maximum size-resolved AR shown in the top right panel of Fig. 2 is less than 0.6 at all supersaturation levels for particles with D_p > 300 nm. This illustrates the impact of local primary particle sources (e.g., emissions generated during cooking time) on CCN activation.

In Case 2 (blue line in Fig. 3), air parcels moved rapidly from the west to the site. The site should then be influenced by the large-scale transportation of air masses. For this case, aerosols contain a small amount of organics (< 30 %), but have high f_{44} (~ 14 %) and κ_{chem} values (~ 0.5). The PSD showed a double peak mode with an N_{CN} of $\sim 1.3 \times 10^4$ cm^{-3} and a relatively high mass concentration of PM_1 (81.45 µg m^{-3}). The double peak mode suggests that aerosols in this case are a mixture of aerosols from local sources and from other regions (Whitby, 1978; Dal Maso et al., 2007). Because aerosols are aged and oxidized during long-distance transport, these particles are usually composed of secondary organic and inorganic components with more hygroscopicity (Weber et al., 1999; Verver et al., 2000). These aerosols can activate efficiently. The maximum AR is close to 1 and the slopes of AR around D_{cut} are steep at all supersaturation levels (middle right panel of Fig. 2). This CCN efficiency spectrum is similar to the ideal spectrum of pure ammonium sulfate.

In Case 3 (green line in Fig. 3), air parcels travelled from the northwest to the site. Air masses arriving at the site in this case had passed over densely populated regions with more heavy pollution. A gradual increase in size-resolved AR with D_p is seen (bottom right panel of Fig. 2). This is attributed to the diversity in aerosol hygroscopicity because of the complex nature of the chemical composition of aerosol particles.

4.3 Estimation of CCN

Precise quantification of N_{CCN} is crucial for understanding aerosol indirect effects and characterizing these effects in models. A CCN closure study is useful to examine the controlling physical and chemical factors and to help verify experimental results. N_{CCN} is usually derived from measured aerosol properties, such as particle number size distribution and composition or hygroscopicity based on the Köhler theory. The closure between measured and estimated N_{CCN} is often achieved under background atmospheric conditions without heavy pollution (Stroud et al., 2007; Bougiatioti et al., 2009). Achieving such closure under heavily polluted conditions is more challenging. In this

section, we investigate the influences of particle physical and chemical properties on N_{CCN} prediction with a focus on particles containing large amounts of organics.

4.3.1 Can we use N_{CN} to parameterize N_{CCN}?

Different parameterizations for estimating CCN have been proposed. A parameterization with very few constants that uses only CCN supersaturation spectra is a simple way to predict CCN number concentrations (Twomey, 1959; Ji and Shaw, 1998; Mircea et al., 2005). These schemes assume a uniform aerosol chemical composition and do not take into account any variation in CCN loading. Bulk ARs have also been used to parameterize CCN number concentrations (Pruppacher and Klett, 1997). However, this method has its limitations because of the spatial variation in AR for maritime and continental aerosols. These variations are primarily attributed to variations in aerosol particle size, i.e., the shape of the PSD as well as particle composition. Empirical formulas and bulk CCN ARs cannot represent CCN spectra in models focused on the North China Plain where there is heavy pollution (Deng et al., 2013). The study by Zhang et al. (2014) demonstrated that the relationship between bulk ARs and N_{CN} is complex under polluted conditions and is heavily dependent on the physicochemical properties of atmospheric aerosols.

Figure 4 shows N_{CN} as a function of N_{CCN} for different supersaturation levels at the Xinzhou and Xianghe sites. As expected, there is a moderate correlation at high supersaturation levels (e.g., R^2 = 0.51 at Xinzhou and R^2 = 0.85 at Xianghe at a supersaturation level of 0.8 %) and a poor correlation at low supersaturation levels. The negative correlation at low supersaturation levels suggests that CCN spectra are not well represented at low supersaturation levels.

4.3.2 Influence of the PSD on N_{CCN} estimation

To investigate the influence of the variation in size distribution on N_{CCN}, the measured CCN efficiency spectrum is multiplied by the mean measured CN size distribution,

which yields the CCN size distribution. This is then integrated over the whole size range (14–600 nm) to estimate N_{CCN}. Figure 5 shows estimated N_{CCN} as a function of observed N_{CCN}. The correlation is poor at all supersaturation levels, with mean slope of 0.80 and R^2 of 0.35. There is little dependency of changes in predicted N_{CCN} at a given supersaturation level to changes in observed N_{CCN}, suggesting the significant influence of the variation in PSD on estimating N_{CCN}.

4.3.3 Impact of x_{org} on N_{CCN}

For the purpose of examining the sensitivity of calculated N_{CCN} to x_{org}, N_{CCN} at three supersaturation levels (0.13, 0.17, and 0.76 %) and three values of x_{org} (35, 52, and 66 %) were computed from CCN efficiency spectra and measured dry particle size distributions. Calculated N_{CCN} were more sensitive to x_{org} at lower supersaturation levels (Fig. 6a and b). At the supersaturation level of 0.13 %, the predicted N_{CCN} was underestimated by 52 % when x_{org} = 66 %, while N_{CCN} was slightly overestimated (~ 3 %) when x_{org} = 35 %. At the supersaturation level of 0.76 % (Fig. 6c), the predicted N_{CCN} was underestimated by 13 % when x_{org} = 66 %. A good agreement is seen when x_{org} = 35 % (R^2 = 0.94). This is likely because a large fraction of particles was already CCN-active. Also, particle composition has relatively less influence on CCN activation at high supersaturation levels (Twohy and Anderson, 2008).

The sensitivity of organics to N_{CCN} increased with increasing x_{org} (Fig. 7). A near-zero bias in the estimate of N_{CCN} is seen when x_{org} = ~ 35 %. This is because this optimal x_{org} is closest in value to the average x_{org} measured during the campaign. If x_{org} is less than the optimal x_{org}, N_{CCN} is overestimated, and vice versa. The bias is more negative as x_{org} increases, suggesting that N_{CCN} is increasingly underestimated, especially at low supersaturations.

When x_{org} is less than 30 %, the overall hygroscopicity of internally mixed particles is dominated by inorganic species such as sulfate and nitrate, which are more hygroscopic than organic compounds with an overall κ_{chem} of 0.46 (κ_{org} = 0.19). As a result,

a larger fraction of particles can be activated. Calculated N_{CCN} would then be greater than measured N_{CCN}. If x_{org} is greater than 60 %, organics will dominate the overall particle hygroscopicity. Particles with a large x_{org} are less hygroscopic and thus are difficult to activate, leading to an overestimation of N_{CCN}. Mei et al. (2013a) observed that N_{CCN} at an urban site was underestimated by ~ 40 % when 60 % < x_{org} < 68 % at a given supersaturation level. This underestimation is less than that observed in this study, i.e., an underestimation in N_{CCN} of 52 % when x_{org} = 66 %. This may be because the measurements described by Mei et al. (2013a) were made in an urban area (~ 60 km downwind of Sacramento, California) where hydrophobic particles would quickly become internal mixtures and hydrophilic by condensation of secondary hygroscopic species (Riemer et al., 2004; Moffet and Prather, 2009; Mei et al., 2013b). The aerosol composition in this case would become increasingly more homogeneous as particles age than those particles observed in suburban areas like Xinzhou. The discrepancy between our estimation and the result reported by Mei et al. (2013a) indicates that increasing the proportion of secondary organics may decrease the uncertainties in predicting N_{CCN} and would lead to a more accurate estimation of N_{CCN}.

4.3.4 Applicability of CCN efficiency spectra

As a means of testing the applicability of the CCN activation spectra, campaign mean CCN efficiency spectra observed at the Xinzhou site is used to estimate N_{CCN} at the Xinzhou and Xianghe sites, which helps to further examine the sensitivity of CCN to aerosol type. Data from the two sites were measured during the warm season so that the effect of temporal variations in aerosols on CCN levels is reduced. First, mean CCN efficiency spectra derived from size-resolved CCN measurements made from 22 July to 26 August 2014 at Xinzhou (corresponding to spectra in Fig. 1) is multiplied by dry CN size distributions measured from 22 July to 26 August 2014 at the Xinzhou site and from 7–22 July 2013 at the Xianghe site. This generates CCN size distributions at the two sites. They are then integrated over the whole size range (14–600 and 10–700 nm at the Xinzhou and Xianghe sites, respectively) to estimate total CCN concentrations.

Figure 8 shows estimated N_{CCN} as a function of measured N_{CCN} for different supersaturation levels at the two sites. N_{CCN} at Xinzhou was underestimated by 4–5 % at supersaturation levels of 0.39 and 0.76 %, and was slightly overestimated (∼ 2 %) at Xianghe for the same supersaturation levels. Good agreement is seen at the 0.39 and 0.76 % supersaturation levels for data from both sites ($R^2 > 0.92$). N_{CCN} at Xinzhou was underestimated by ∼ 7 % at supersaturation levels < 0.1 % ($R^2 = 0.87$). At Xianghe, however, N_{CCN} was overestimated by 19–23 % at supersaturation levels < 0.1 % although the correlation between calculated and measured N_{CCN} was good. Because size-resolved CCN efficiency spectra were applied here, excluding the impact of particle size, the influence of chemical composition on CCN activation can be investigated. The poor estimates of CCN at low supersaturation levels could be attributed to the high sensitivity of N_{CCN} to chemical composition. Because the mass fractions of inorganics and organics measured at the two sites are similar (Fig. 1) and the hygroscopicity for inorganic components is fixed, this overestimation is attributed to the smaller proportion of aged and oxidized organic aerosols at Xianghe compared with aerosols at Xinzhou (f_{44} = 17 and 11 % at Xinzhou and Xianghe, respectively).

5 Summary and conclusions

In this study, we have investigated the complexity of parameterizing CCN when changes in particle physicochemical properties occur based on field measurements obtained from 22 July to 26 August of 2014 in the suburb of Xinzhou, China. Five-day back trajectories combined with measurements were analyzed to examine air mass influences on CCN activity. CCN efficiency was largely reduced by local primary biomass burning events during which high N_{CN} (∼ 1.7×10^4 cm^{-3}, PM_1 = 28.36 µg m^{-3}) and high x_{org} (> 60 %) were measured. f_{44} was equal to ∼ 10 % and $\kappa_{chem} < 0.3$. The PSD showed a single peak mode at D_p = 56 nm. Aerosol particles were efficiently activated when the site was influenced by regional air masses, but less efficiently activated when aerosols were mainly composed of organics.

The relationship between N_{CN} and N_{CCN} was generally poor. Large errors would arise if using the former to estimate the latter, especially under low supersaturation conditions. The PSD was found to play a dominant role in N_{CCN}, which also showed a strong dependence on x_{org}. This dependence weakens as the supersaturation level increases. N_{CCN} was underestimated by 52 and 13 % at supersaturation levels of 0.13 and 0.76 %, respectively, when x_{org} = 66 %. The agreement is better when x_{org} is reduced to 35 % ($R^2 = 0.94$).

The applicability of the CCN efficiency spectrum measured at the Xinzhou site to the Xianghe site was examined and a good agreement was found when the supersaturation level was > 0.2 %. However, N_{CCN} at the Xianghe site was overestimated by 19–23 % when the supersaturation level was < 0.1 %. Because of the similar mass fractions of inorganics and organics measured at the two sites, we conclude that this overestimation was mainly caused by the smaller proportion of aged and oxidized organic aerosols at Xianghe compared with aerosols at Xinzhou.

Acknowledgements. This work was funded by the National Basic Research Program of China "973" (Grant No. 2013CB955801, 2013CB955804), the Fundamental Research Funds for the Central Universities (Grant No. 2013YB35) and the NSCF-TAMU Collaborative Research Grant Program (Grant No. 4141101031). We also acknowledge the members of the A^2C^2 team for their hard work during the campaign, including Du Wei (from the State Key Laboratory of Atmospheric Boundary Layer Physics and Atmospheric Chemistry of the Institute of Atmospheric Physics/Chinese Academy of Sciences for carrying out the chemical composition measurements) and Yuan Cheng (from Nanjing University who helped make the size-resolved CCNc measurements). Thank Mr. Mcribb's assistance in correction the English.

References

Aiken, A. C., DeCarlo, P. F., Kroll, J. H., Worsnop, D. R., Huffman, J. A., Docherty, K. S., Ulbrich, I. M., Mohr, C., Kimmel, J. R., Sueper, D., Sun, Y., Zhang, Q., Trimborn, A., Northway, M., Ziemann, P. J., Canagaratna, M. R., Onasch, T. B., Alfarra, M. R., Prevot, A. S. H., Dommen, J., Duplissy, J., Metzger, A., Baltensperger, U., and Jimenez, J. L.: O / C and

OM / OC ratios of primary, secondary, and ambient organic aerosols with high-resolution time-of-flight aerosol mass spectrometry, Environ. Sci. Technol., 42, 4478–4485, 2008.
Bougiatioti, A., Fountoukis, C., Kalivitis, N., Pandis, S. N., Nenes, A., and Mihalopoulos, N.: Cloud condensation nuclei measurements in the marine boundary layer of the Eastern Mediterranean: CCN closure and droplet growth kinetics, Atmos. Chem. Phys., 9, 7053–7066, doi:10.5194/acp-9-7053-2009, 2009.
Bougiatioti, A., Nenes, A., Fountoukis, C., Kalivitis, N., Pandis, S. N., and Mihalopoulos, N.: Size-resolved CCN distributions and activation kinetics of aged continental and marine aerosol, Atmos. Chem. Phys., 11, 8791–8808, doi:10.5194/acp-11-8791-2011, 2011.
Chuang, P. Y., Collins, D. R., Pawlowska, H., Snider, J. R., Jonsson, H. H., Brenguier, J. L., Flagan, R. C., and Seinfeld, J. H.: CCN measurements during ACE-2 and their relationship to cloud microphysical properties, Tellus B, 52, 843–867, 2000.
Clarke, A., McNaughton, C., Kasputin, V. N., Shinozuka, Y., Howell, S., Dibb, J., Zhou, J., Anderson, B., Brekhovskikh, V., Turner, H., and Pinkerton, M.: Biomass burning and pollution aerosol over North America: organic components and their influence on spectral optical properties and humidification response, J. Geophys. Res., 112, D12S18, doi:10.1029/2006JD007777, 2007.
Dal Maso, M., Sogacheva, L., Aalto, P. P., Riipinen, I., Komppula, M., Tunved, P., Korhonen, L., Suur-Uski, V., Hirsikko, A., Kurten, T., Kerminen, V. M., Lihavainen, H., Viisanen, Y., Hansson, H.-C., and Kulmala, M.: Aerosol size distribution measurements at four Nordic field stations: identification, analysis and trajectory analysis of new particle formation bursts, Tellus B, 59, 350–361, 2007.
Deng, Z. Z., Zhao, C. S., Ma, N., Liu, P. F., Ran, L., Xu, W. Y., Chen, J., Liang, Z., Liang, S., Huang, M. Y., Ma, X. C., Zhang, Q., Quan, J. N., Yan, P., Henning, S., Mildenberger, K., Sommerhage, E., Schäfer, M., Stratmann, F., and Wiedensohler, A.: Size-resolved and bulk activation properties of aerosols in the North China Plain, Atmos. Chem. Phys., 11, 3835–3846, doi:10.5194/acp-11-3835-2011, 2011.
Deng, Z. Z., Zhao, C. S., Ma, N., Ran, L., Zhou, G. Q., Lu, D. R., and Zhou, X. J.: An examination of parameterizations for the CCN number concentration based on in situ measurements of aerosol activation properties in the North China Plain, Atmos. Chem. Phys., 13, 6227–6237, doi:10.5194/acp-13-6227-2013, 2013.
Draxler, R. R. and Hess, G. D.: An overview of the HYSPLIT 4 modeling system for trajectories, dispersion, and deposition, Aust. Meteorol. Mag., 47, 295–308, 1998.

Duplissy, J., DeCarlo, P. F., Dommen, J., Alfarra, M. R., Metzger, A., Barmpadimos, I., Prevot, A. S. H., Weingartner, E., Tritscher, T., Gysel, M., Aiken, A. C., Jimenez, J. L., Canagaratna, M. R., Worsnop, D. R., Collins, D. R.,Tomlinson, J., and Baltensperger, U.: Relating hygroscopicity and composition of organic aerosol particulate matter, Atmos. Chem. Phys., 11, 1155–1165, doi:10.5194/acp-11-1155-2011, 2011.
Dusek, U., Covert, D. S., Wiedensohler, A., Neususs, C., Weise, D., and Cantrell, W.: Cloud condensation nuclei spectra derived from size distributions and hygroscopic properties of the aerosol in coastal south-west Portugal during ACE-2, Tellus B, 55, 35–53, 2003.
Engelhart, G. J., Hennigan, C. J., Miracolo, M. A., Robinson, A. L., and Pandis, S. N.: Cloud condensation nuclei activity of fresh primary and aged biomass burning aerosol, Atmos. Chem. Phys., 12, 7285–7293, doi:10.5194/acp-12-7285-2012, 2012.
Ervens, B., Cubison, M. J., Andrews, E., Feingold, G., Ogren, J. A., Jimenez, J. L., Quinn, P. K., Bates, T. S., Wang, J., Zhang, Q., Coe, H., Flynn, M., and Allan, J. D.: CCN predictions using simplified assumptions of organic aerosol composition and mixing state: a synthesis from six different locations, Atmos. Chem. Phys., 10, 4795–4807, doi:10.5194/acp-10-4795-2010, 2010.
Gasparini, R., Collins, D. R., Andrews, E., Sheridan, P. J., Ogren, J. A., and Hudson, J. G.: Coupling aerosol size distributions and size-resolved hygroscopicity to predict humidity-dependent optical properties and cloud condensation nuclei spectra, J. Geophys. Res., 111, D05S13, doi:10.1029/2005JD006092, 2006.
Gunthe, S. S., Rose, D., Su, H., Garland, R. M., Achtert, P., Nowak, A., Wiedensohler, A., Kuwata, M., Takegawa, N., Kondo, Y., Hu, M., Shao, M., Zhu, T., Andreae, M. O., and Pöschl, U.: Cloud condensation nuclei (CCN) from fresh and aged air pollution in the megacity region of Beijing, Atmos. Chem. Phys., 11, 11023–11039, doi:10.5194/acp-11-11023-2011, 2011.
Guo, S., Hu, M., Zamor, M. L., Peng, J., Shang, D., Zheng, J., Du, Z., Wu, Z., Shao, M., Zeng, L., Molina, M. J., and Zhang, R.: Elucidating severe urban haze formation in China, P. Natl. Acad. Sci. USA, 111, 17373–17378, doi:10.1073/pnas.1419604111, 2014.
Hartz, K. E. H., Tischuk, J. E., Chan, M. N., Chan, C. K., Donahue, N. M., and Pandis, S. N.: Cloud condensation nuclei activation of limited solubility organic aerosol, Atmos. Environ., 40, 605–617, 2006.
Hings, S. S., Wrobel, W. C., Cross, E. S., Worsnop, D. R., Davidovits, P., and Onasch, T. B.: CCN activation experiments with adipic acid: effect of particle phase and adipic acid coatings

on soluble and insoluble particles, Atmos. Chem. Phys., 8, 3735–3748, doi:10.5194/acp-8-3735-2008, 2008.
Hudson, J. G. and Da, X. Y.: Volatility and size of cloud condensation nuclei, J. Geophys. Res., 101, 4435–4442, 1996.
Hussein, T., Dal Maso, M., Petäjä, T., Koponen, I. K., Paatero, P., Aalto, P. P., Hämeri, K., and Kulmala, M.: Evaluation of an automatic algorithm for fitting the particle number size distributions, Boreal Environ. Res., 10, 337–355, 2005.
Ji, Q. and Shaw, G. E.: On supersaturation spectrum and size distributions of cloud condensation nuclei, Geophys. Res. Lett., 25, 1903–1906, doi:10.1029/98gl01404, 1998.
Junge, C. and McLaren, E.: Relationship of cloud nuclei spectra to aerosol size distribution and composition, J. Atmos. Sci., 28, 382–390, 1971.
Kammermann, L., Gysel, M., Weingartner, E., Herich, H., Cziczo, D. J., Holst, T., Svenningsson, B., Arneth, A., and Baltensperger, U.: Subarctic atmospheric aerosol composition: 3. Measured and modeled properties of cloud condensation nuclei, J. Geophys. Res., 115, D04202, doi:10.1029/2009JD012447, 2010.
Köhler, H.: The nucleus in and growth of hygroscopic droplets, T. Faraday Soc., 32, 1152–1161, doi:10.1039/TF9363201152, 1936.
Lance, S., Medina, J., Smith, J., and Nenes, A.: Mapping the operation of the DMT continuous flow CCN counter, Aerosol Sci. Tech., 40, 242–254, 2006.
Lathem, T. L., Beyersdorf, A. J., Thornhill, K. L., Winstead, E. L., Cubison, M. J., Hecobian, A., Jimenez, J. L., Weber, R. J., Anderson, B. E., and Nenes, A.: Analysis of CCN activity of Arctic aerosol and Canadian biomass burning during summer 2008, Atmos. Chem. Phys., 13, 2735–2756, doi:10.5194/acp-13-2735-2013, 2013.
Lee, Y. S., Collins, D. R., Li, R. J., Bowman, K. P., and Feingold, G.: Expected impact of an aged biomass burning aerosol on cloud condensation nuclei and cloud droplet concentrations, J. Geophys. Res., 111, D22204, doi:10.1029/2005JD006464, 2006.
Li, Z., Chen, H., Cribb, M., Dickerson, R. E., Holben, B., Li, C., Lu, D., Luo, Y., Maring, H., Shi, G., Tsay, S.-C., Wang, P., Wang, Y., Xia, X., Zheng, Y., Yuan, T., and Zhao, F.: Preface to special section on East Asian Studies of Tropospheric Aerosols: an International Regional Experiment (EASTAIRE), J. Geophys. Res., 112, D22S00, doi:10.1029/2007JD008853, 2007.
Li, Z., Li, C., Chen, H., Tsay, S.-C., Holben, B., Huang, J., Li, B., Maring, H., Qian, Y., Shi, G., Xia, X., Yin, Y., Zheng, Y., and Zhuang, G.: East Asian Studies of Tropospheric Aerosols

and Impact on Regional Climate (EAST-IRC): an overview, J. Geophys. Res., 116, D00K34, doi:10.1029/2010JD015257, 2011.
Liu, X. and Wang, J.: How important is organic aerosol hygroscopicity to aerosol indirect forcing?, Environ. Res. Lett., 5, 044010, doi:10.1088/1748-9326/5/4/044010, 2010.
McFiggans, G., Artaxo, P., Baltensperger, U., Coe, H., Facchini, M. C., Feingold, G., Fuzzi, S., Gysel, M., Laaksonen, A., Lohmann, U., Mentel, T. F., Murphy, D. M., O'Dowd, C. D., Snider, J. R., and Weingartner, E.: The effect of physical and chemical aerosol properties on warm cloud droplet activation, Atmos. Chem. Phys., 6, 2593–2649, doi:10.5194/acp-6-2593-2006, 2006.
Mei, F., Setyan, A., Zhang, Q., and Wang, J.: CCN activity of organic aerosols observed downwind of urban emissions during CARES, Atmos. Chem. Phys., 13, 12155–12169, doi:10.5194/acp-13-12155-2013, 2013a.
Mei, F., Hayes, P. L., Ortega, A. M., Taylor, J. W., Allan, J. D., Gilman, J. B., Kuster, W. C., de Gouw, J. A., Jimenez, J. L., and Wang, J.: Droplet activation properties of organic aerosols observed at an urban site during CalNex-LA, J. Geophys. Res., 118, 2903–2917, doi:10.1002/jgrd.50285, 2013b.
Mikhailov, E., Vlasenko, S., Martin, S. T., Koop, T., and Pöschl, U.: Amorphous and crystalline aerosol particles interacting with water vapor: conceptual framework and experimental evidence for restructuring, phase transitions and kinetic limitations, Atmos. Chem. Phys., 9, 9491–9522, doi:10.5194/acp-9-9491-2009, 2009.
Mircea, M., Facchini, M. C., Decesari, S., Cavalli, F., Emblico, L., Fuzzi, S., Vestin, A., Rissler, J., Swietlicki, E., Frank, G., Andreae, M. O., Maenhaut, W., Rudich, Y., and Artaxo, P.: Importance of the organic aerosol fraction for modeling aerosol hygroscopic growth and activation: a case study in the Amazon Basin, Atmos. Chem. Phys., 5, 3111–3126, doi:10.5194/acp-5-3111-2005, 2005.
Moffet, R. C. and Prather, K. A.: In-situ measurements of the mixing state and optical properties of soot with implications for radiative forcing estimates, P. Natl. Acad. Sci. USA, 106, 11872–11877, 2009.
Ng, N. L., Herndon, S. C., Trimborn, A., Canagaratna, M. R., Croteau, P. L., Onasch, T. B., Sueper, D., Worsnop, D. R., Zhang, Q., Sun, Y. L., and Jayne, J. T.: An Aerosol Chemical Speciation Monitor (ACSM) for Routine Monitoring of the Composition and Mass Concentrations of Ambient Aerosol, Aerosol Sci. Tech., 45, 770–784, 2011.

Niedermeier, D., Wex, H., Voigtländer, J., Stratmann, F., Brüggemann, E., Kiselev, A., Henk, H., and Heintzenberg, J.: LACIS-measurements and parameterization of sea-salt particle hygroscopic growth and activation, Atmos. Chem. Phys., 8, 579–590, doi:10.5194/acp-8-579-2008, 2008.
Paramonov, M., Aalto, P. P., Asmi, A., Prisle, N., Kerminen, V.-M., Kulmala, M., and Petäjä, T.: The analysis of size-segregated cloud condensation nuclei counter (CCNC) data and its implications for cloud droplet activation, Atmos. Chem. Phys., 13, 10285–10301, doi:10.5194/acp-13-10285-2013, 2013.
Petters, M. D. and Kreidenweis, S. M.: A single parameter representation of hygroscopic growth and cloud condensation nucleus activity, Atmos. Chem. Phys., 7, 1961–1971, doi:10.5194/acp-7-1961-2007, 2007.
Petters, M. D. and Kreidenweis, S. M.: A single parameter representation of hygroscopic growth and cloud condensation nucleus activity – Part 2: Including solubility, Atmos. Chem. Phys., 8, 6273–6279, doi:10.5194/acp-8-6273-2008, 2008.
Pruppacher, H. R. and Klett, J. D.: Microphysics of Clouds and Precipitation, Kluwer Academic Publishers, Dordrecht, the Netherlands, 944 pp., 1997.
Raymond, T. M. and Pandis, S. N.: Cloud activation of single component organic aerosol particles, J. Geophys. Res., 107, 4787, doi:10.1029/2002JD002159, 2002.
Reutter, P., Su, H., Trentmann, J., Simmel, M., Rose, D., Gunthe, S. S., Wernli, H., Andreae, M. O., and Pöschl, U.: Aerosol- and updraft-limited regimes of cloud droplet formation: influence of particle number, size and hygroscopicity on the activation of cloud condensation nuclei (CCN), Atmos. Chem. Phys., 9, 7067–7080, doi:10.5194/acp-9-7067-2009, 2009.
Riemer, N., Vogel, H., and Vogel, B.: Soot aging time scales in polluted regions during day and night, Atmos. Chem. Phys., 4, 1885–1893, doi:10.5194/acp-4-1885-2004, 2004.
Rissler, J., Swietlicki, E., Zhou, J., Roberts, G., Andreae, M. O., Gatti, L. V., and Artaxo, P.: Physical properties of the sub-micrometer aerosol over the Amazon rain forest during the wet-to-dry season transition - comparison of modeled and measured CCN concentrations, Atmos. Chem. Phys., 4, 2119–2143, doi:10.5194/acp-4-2119-2004, 2004.
Rissler, J., Vestin, A., Swietlicki, E., Fisch, G., Zhou, J., Artaxo, P., and Andreae, M. O.: Size distribution and hygroscopic properties of aerosol particles from dry-season biomass burning in Amazonia, Atmos. Chem. Phys., 6, 471–491, doi:10.5194/acp-6-471-2006, 2006.
Rose, D., Gunthe, S. S., Mikhailov, E., Frank, G. P., Dusek, U., Andreae, M. O., and Pöschl, U.: Calibration and measurement uncertainties of a continuous-flow cloud condensation nuclei

counter (DMT-CCNC): CCN activation of ammonium sulfate and sodium chloride aerosol particles in theory and experiment, Atmos. Chem. Phys., 8, 1153–1179, doi:10.5194/acp-8-1153-2008, 2008.
Rose, D., Nowak, A., Achtert, P., Wiedensohler, A., Hu, M., Shao, M., Zhang, Y., Andreae, M. O., and Pöschl, U.: Cloud condensation nuclei in polluted air and biomass burning smoke near the mega-city Guangzhou, China – Part 1: Size-resolved measurements and implications for the modeling of aerosol particle hygroscopicity and CCN activity, Atmos. Chem. Phys., 10, 3365–3383, doi:10.5194/acp-10-3365-2010, 2010.
Rousseau, D. D., Duzer, D., Etienne, J., L., Cambon, G., Jolly, D., Ferrier, J., and Schevin, P.: Pollen record of rapidly changing air trajectories to the North Pole, J. Geophys. Res., 109, D06116, doi:10.1029/2003JD003985, 2004.
Sotiropoulou, R. E. P., Nenes, A., Adams, P. J., and Seinfeld, J. H.: Cloud condensation nuclei prediction error from application of Köhler theory: importance for the aerosol indirect effect, J. Geophys. Res., 112, D12202, doi:10.1029/2006JD007834, 2007.
Stohl, A.: Trajectory statistics – a new method to establish source-receptor relationships of air pollutants and its application to the transport of particulate sulfate in Europe, Atmos. Environ., 30, 579–587, 1996.
Stroud, C. A., Nenes, A., Jimenez, J. L., DeCarlo, P., Huffman, J. A., Bruintjes, R., Nemitz, E., Delia, A. E., Toohey, D. W., Guenther, A. B., and Nandi, S.: Cloud Activating Properties of Aerosol Observed during CELTIC, J. Atmos. Sci., 64, 441–459, 2007.
Sun, Y., Wang, Z., Dong, H., Yang, T., Li, J., Pan, X., Chen, P., and Jayne, J. T.: Characterization of summer organic and inorganic aerosols in Beijing, China with an Aerosol Chemical Speciation Monitor, Atmos. Environ., 51, 250–259, doi:10.1016/j.atmosenv.2012.01.013, 2012.
Takegawa, N., Miyakawa, T., Kawamura, K., and Kondo, Y.: Contribution of selected di-carboxylic and omega-oxocarboxylic acids in ambient aerosol to the m/z 44 signal of an aerodyne aerosol mass spectrometer, Aerosol Sci. Tech., 41, 418–437, doi:10.1080/02786820701203215, 2007.
Turpin, B. J. and Lim, H. J.: Species contributions to $PM_{2.5}$ mass concentrations: revisiting common assumptions for estimating organic mass, Aerosol Sci. Tech., 35, 602–610, 2001.
Twohy, C. H. and Anderson, J. R.: Droplet nuclei in non-precipitating clouds: composition and size matter, Environ. Res. Lett., 3, 045002, doi:10.1088/1748-9326/3/4/045002, 2008.
Twomey, S.: The nuclei of natural cloud formation part II: The supersaturation in natural clouds and the variation of cloud droplet concentration, Pure Appl. Geophys., 43, 243–249, 1959.

VanReken, T. M., Rissman, T. A., Roberts, G. C., Varutbangkul, V., Jonsson, H. H., Flagan, R. C., and Seinfeld, J. H.: Toward aerosol/cloud condensation nuclei (CCN) closure during CRYSTAL-FACE, J. Geophys. Res., 108, 4633, doi:10.1029/2003JD003582, 2003.

VanReken, T. M., Ng, N. L., Flagan, R. C., and Seinfeld, J. H.: Cloud condensation nucleus activation properties of biogenic secondary organic aerosol, J. Geophys. Res., 110, D07206, doi:10.1029/2004JD005465, 2005.

Varutbangkul, V., Brechtel, F. J., Bahreini, R., Ng, N. L., Keywood, M. D., Kroll, J. H., Flagan, R. C., Seinfeld, J. H., Lee, A., and Goldstein, A. H.: Hygroscopicity of secondary organic aerosols formed by oxidation of cycloalkenes, monoterpenes, sesquiterpenes, and related compounds, Atmos. Chem. Phys., 6, 2367–2388, doi:10.5194/acp-6-2367-2006, 2006.

Verver, G., Raes, F., Vogelezang, D., and Johnson, D.: The 2nd Aerosol characterization Experiment (ACE-2): meteorological and chemical context, Tellus B, 52, 126–140, 2000.

Wang, J., Lee, Y.-N., Daum, P. H., Jayne, J., and Alexander, M. L.: Effects of aerosol organics on cloud condensation nucleus (CCN) concentration and first indirect aerosol effect, Atmos. Chem. Phys., 8, 6325–6339, doi:10.5194/acp-8-6325-2008, 2008.

Wang, Y. Q., Zhang, X. Y., and Draxler, R.: TrajStat: GIS-based software that uses various trajectory statistical analysis methods to identify potential sources from long-term air pollution measurement data, Environ. Modell. Softw., 24, 938–939, 2009.

Ward, D. S., Eidhammer, T., Cotton, W. R., and Kreidenweis, S. M.: The role of the particle size distribution in assessing aerosol composition effects on simulated droplet activation, Atmos. Chem. Phys., 10, 5435–5447, doi:10.5194/acp-10-5435-2010, 2010.

Weber, R., McMurry, P. H., Mauldin, R., Tanner, D., Eisele, F., Clarke, A., and Kapustin, V.: New particle formation in the remote troposphere: a comparison of observations at various sites, Geophys. Res. Lett., 26, 307–310, 1999.

Wex, H., Hennig, T., Salma, I., Ocskay, R., Kiselev, A., Henning, S.,Massling, A., Wiedensohler, A., and Stratmann, F.: Hygroscopic growth and measured and modeled critical super-saturations of an atmospheric HULIS sample, Geophys. Res. Lett., 34, L02818, doi:10.1029/2006GL028260, 2007.

Whitby, K. T.: The physical characteristics of sulfur aerosols, Atmos. Environ., 12, 135–159, 1967, online publication date 1 January 1978.

Wiedensohler, A., Cheng, Y. F., Nowak, A., Wehner, B., Achtelt, P., Berghof, M., Birmili, W., Wu, Z. J., Hu, M., Zhu, T., Takegawa, N., Kita, K., Kondo, Y., Lou, S. R., Hofeumahaus, A., Holland, F., Wahner, A., Gunthe, S. S., Rose, D., Su, H., and Pöschl, U.: Rapid aerosol

particle growth and increase of cloud condensation nucleus activity by secondary aerosol formation and condensation: a case study for regional air pollution in northeastern China, J. Geophys. Res.-Atmos., 114, D00G08, doi:10.1029/2008JD010884, 2009.

Yue, D. L., Hu, M., Zhang, R. J., Wu, Z. J., Su, H., Wang, Z. B., Peng, J. F., He, L. Y., Huang, X. F., Gong, Y. G., and Wiedensohler, A.: Potential contribution of new particle formation to cloud condensation nuclei in Beijing, Atmos. Environ., 45, 6070–6077, 2011.

Zhang, F., Li, Y., Li, Z., Sun, L., Li, R., Zhao, C., Wang, P., Sun, Y., Liu, X., Li, J., Li, P., Ren, G., and Fan, T.: Aerosol hygroscopicity and cloud condensation nuclei activity during the AC^{3}Exp campaign: implications for cloud condensation nuclei parameterization, Atmos. Chem. Phys., 14, 13423–13437, doi:10.5194/acp-14-13423-2014, 2014.

Zhang, Q., Meng, J., Quan, J., Gao, Y., Zhao, D., Chen, P., and He, H.: Impact of aerosol composition on cloud condensation nuclei activity, Atmos. Chem. Phys., 12, 3783–3790, doi:10.5194/acp-12-3783-2012, 2012.

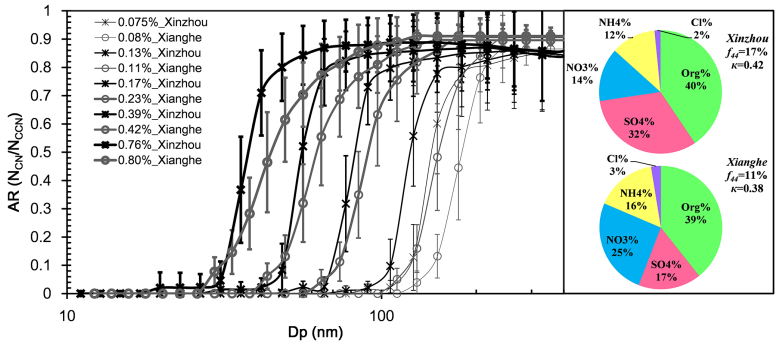

Figure 1. Mean CCN efficiency spectra at the Xinzhou site (black lines with asterisks) measured from 22 July–26 August 2014 and at the Xianghe site (grey lines with circles) site measured from 7–21 July 2013 for different supersaturation levels. Error bars representing one standard deviation are shown. Right panels show particle chemical composition in terms of mass concentration fractions at Xinzhou (top panel) and Xianghe (bottom panel) during their respective observation periods. Note that the preset supersaturation levels were 0.07, 0.1, 0.2, 0.4 and 0.8 % at both sites, but effective supersaturation levels were slightly different after calibration.

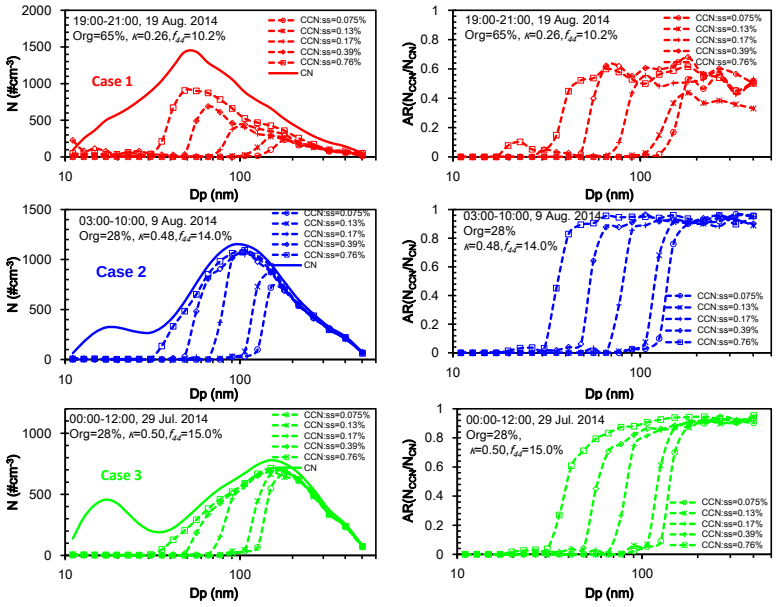

Figure 2. CN and CCN size distributions (left panels) and CCN efficiency spectra (right panels) at different supersaturation levels for Case 1 (upper panels, 19 August 2014, 19:00–21:00 LT), Case 2 (middle panels, 9 August 2014, 03:00–10:00 LT), and Case 3 (bottom panels, 29 July 2014, 00:00–12:00 LT). CN number concentrations are 16 671, 12 869, and 10 134 cm^{-3} for Case 1, Case 2, and Case 3, respectively. Mass concentrations of PM_1 are 28.36, 81.45, and 78.73 $\mu g\,m^{-3}$ for Case 1, Case 2 and Case 3, respectively.

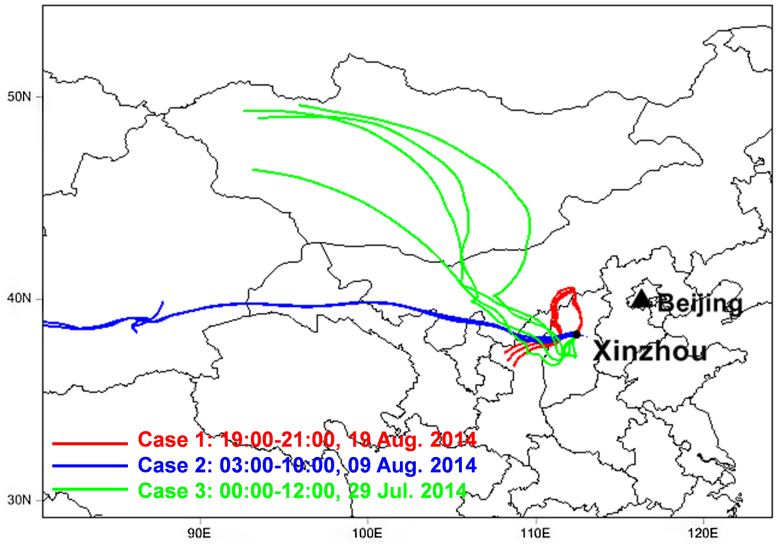

Figure 3. Five-day back trajectories for Case 1 (in red), Case 2 (in blue), and Case 3 (in green) calculated using the Hybrid Single-Particle Lagrangian Integrated Trajectory model with National Centers for Environmental Prediction reanalysis data. The arrival height of the trajectories at the Xinzhou site was at the surface.

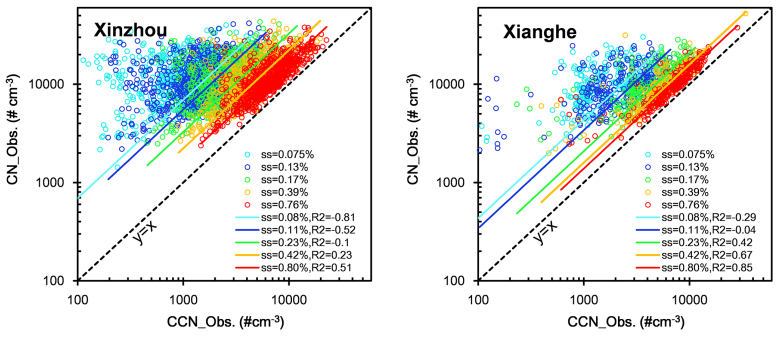

Figure 4. Measured N_{CN} as a function of measured N_{CCN} for different supersaturation levels at the Xinzhou (left panel) and Xianghe (right panel) sites.

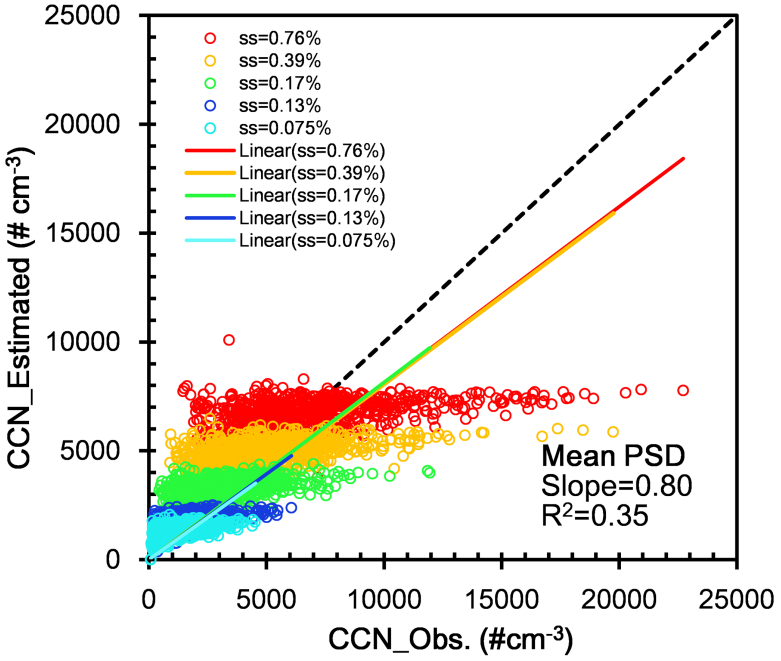

Figure 5. Estimated N_{CCN} as a function of measured N_{CCN} at different supersaturation levels using the campaign mean particle size distribution and measured size-resolved activation ratios (N_{CCN}/N_{CN}). The diagonal dashed line is the 1 : 1 line.

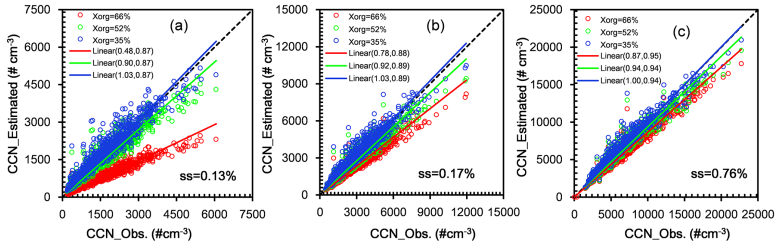

Figure 6. The sensitivity of organics mass fraction (x_{org}) to estimates of N_{CCN} for cases when x_{org} = 35 (blue circles), 52 (green circles), and 66 % (red circles) at supersaturation levels of **(a)** 0.13, **(b)** 0.17, and **(c)** 0.76 %. Mean values of the hygroscopic parameter κ_{chem} are 0.46, 0.34, and 0.26 for the three cases, respectively. Mean values of the hygroscopic parameter κ_{org} are 0.19, 0.13, and 0.08 for the three cases, respectively. Linear best-fit lines through each group of points are shown. Slopes and R^2 values are given in parentheses.

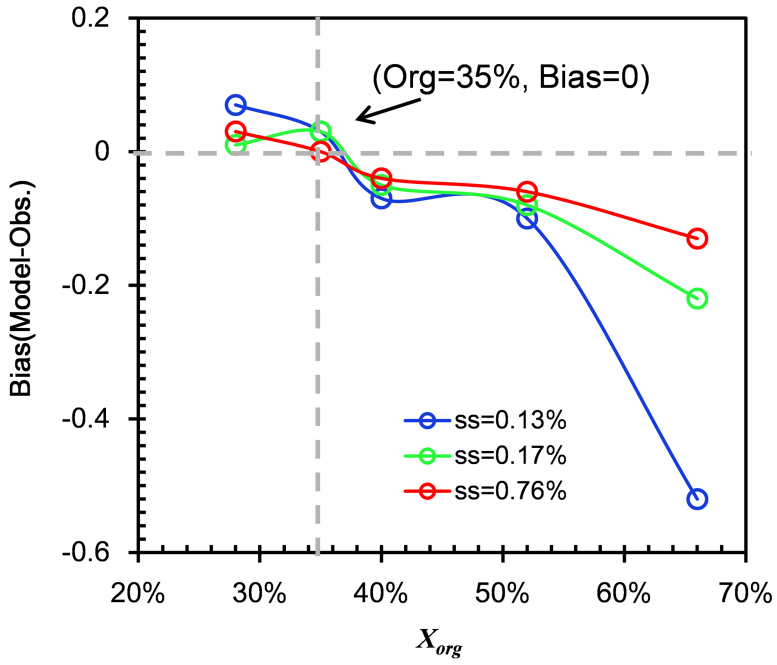

Figure 7. Biases (estimated minus observed N_{CCN}) as a function of mass fraction of organics (x_{org}) at different supersaturation levels.

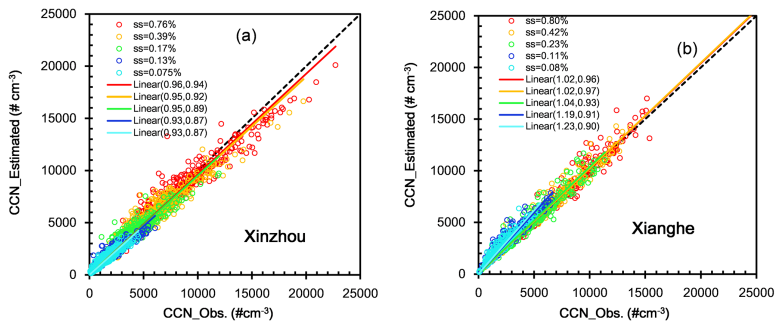

Figure 8. Estimated N_{CCN} as a function of observed N_{CCN} for different supersaturation levels at **(a)** Xinzhou and **(b)** Xianghe. Note that the campaign mean CCN efficiency spectra at Xinzhou are used for estimating N_{CCN} at Xianghe. Linear best-fit lines through each group of points are shown. Slopes and R^2 values are given in parentheses.